Available online at www.sciencedirect.com
SCIENCE DIRECT®
Polymer 46 (2005) 8908–8912
polymer
www.elsevier.com/locate/polymer

Pulsed plasmachemical deposition of polymeric salt networks

C.G. Spanos[a], J.P.S. Badyal[a,*], A.J. Goodwin[b], P.J. Merlin[c]

[a]*Science Laboratories, Department of Chemistry, Durham University, Durham DH1 3LE, England, UK*
[b]*Dow Corning Ltd., Barry CF63 2YL, Wales, UK*
[c]*Dow Corning SA, Parc Industriel, 7180 Seneffe, Belgium*

Received 26 April 2005; received in revised form 29 June 2005; accepted 30 June 2005
Available online 8 August 2005

Abstract

A solventless substrate-independent approach for synthesizing structurally well-defined polymer salt networks onto solid surfaces is described. This entails pulsed plasma co-polymerization of acid and base containing precursors. In the case of acrylic acid and allylamine, one manifestation of the deposited ionic and covalent cross-linked layers is that they promote the formation of a closely packed gas impermeable structure.

Keywords: Polymeric salt; Plasma; Surface

1. Introduction

Thin polymeric salt layers are of potential interest for a wide range of applications (e.g. dielectric films [1], biodegradable coatings [2], printing [3,4], semipermeable membranes [5], chelating agents [6], etc.). In the past, solution-based methods have been mainly employed for this purpose, for instance reacting base molecules with polymeric chains containing pendant acid groups [1], or the polymerisation of acid monomers in combination with base [2]. In this article, we describe an alternative simple, single-step, solventless pulsed plasmachemical methodology for making polymeric salt networks.

Low temperature plasma polymerisation [7] of volatile organic precursors is a well-established technique for depositing functionalised thin films [8]. In recent years it has been shown that pulsing the applied electric field during plasma polymerisation can lead to structurally well-defined polymer repeat units [9,10]. This has been attributed to minimal fragmentation of the monomer and very little damage of the growing film by incident plasma species during the duty cycle on-period (microseconds), followed by conventional polymerisation mechanisms proceeding during the off-period at activated centres (milliseconds). Advantages associated with this method include the fact that the gaseous and reactive nature of the electrical discharge means that it is applicable to a whole host of materials and complex geometries (e.g. microspheres, fibres, tubes, etc.). Examples devised in the past include: Perfluoroalkyl [11], epoxide [12], anhydride [13], carboxylic acid [14], cyano [15], hydroxyl [16], and amine [17] functionalized surfaces. In this article, we show how pulsed plasma co-polymerization of acid and base containing monomers leads to the formation of a crosslinked polymeric salt network. For illustrative purposes, the combination of acrylic acid and allylamine to yield a polymeric network crosslinked by ammonium–carboxylate salt interactions is described in Structures 1 and 2.

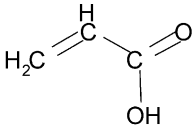

Structure 1: Acrylic acid

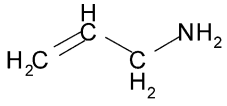

Structure 2: Allylamine

2. Experimental

Acrylic acid (Aldrich, +99% purity) and allylamine (Aldrich, +99% purity) precursors were loaded into

* Corresponding author.
E-mail address: j.p.badyal@durham.ac.uk (J.P.S. Badyal).

0032-3861/$ - see front matter © 2005 Elsevier Ltd. All rights reserved.
doi:10.1016/j.polymer.2005.06.123

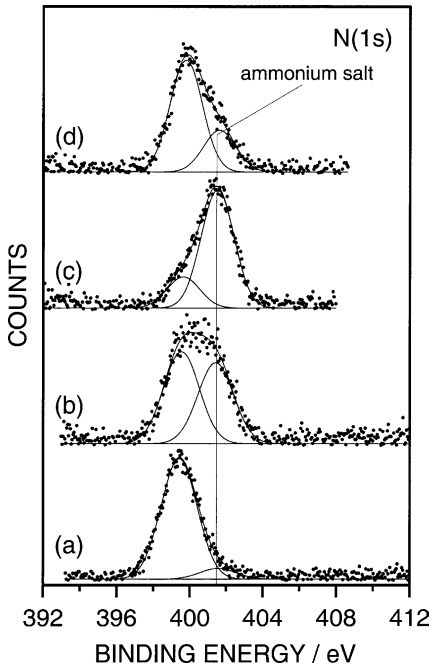

Fig. 1. Quantification of ammonium salt formation using N (1s) XPS analysis: (a) Pulsed allylamine (0.3 mbar), (b) pulsed acrylic acid (0.15 mbar) + allylamine (0.15 mbar), (c) pulsed acrylic acid (0.2 mbar) + allylamine (0.1 mbar), and (d) continuous wave acrylic acid (0.2 mbar) + allylamine (0.1 mbar).

stoppered glass tubes, and further purified by multiple freeze-pump-thaw cycles. Pulsed plasma deposition of the individual monomers and also mixtures was carried out in a cylindrical glass reactor (418 cm^3 volume) which was continuously pumped by a mechanical rotary pump via a liquid nitrogen cold trap (base pressure 8×10^{-3} mbar and 1.61×10^{-8} mol s^{-1} leak rate). A copper coil wrapped around the reactor was coupled to a 13.56 MHz radio frequency (RF) power supply via an LC matching network. The whole system was enclosed in a Faraday cage. Prior to each experiment, the chamber was scrubbed with detergent, rinsed in propan-2-ol, and then cleaned using a 50 W air plasma at 0.2 mbar. The absence of any deposit from the previous experiment was confirmed by XPS analysis. The respective monomer feeds were then introduced via fine control needle valves at a predetermined pressure, followed by ignition of the electrical discharge and film deposition. A signal generator was used to trigger the RF power supply, and the corresponding pulse waveform was monitored with an oscilloscope. The average power $\langle P\rangle$ delivered to the system was calculated using the following expression:

$$\langle P\rangle = P_P\left\{\frac{t_{on}}{(t_{on}+t_{off})}\right\}$$

where P_p is the power output of the RF generator, t_{on} and t_{off} are the pulse on- and off-periods, respectively, and $t_{on}/(t_{on}+t_{off})$ is defined as the duty cycle [18]. Typical conditions were 10 min deposition, with $P_p=10$ W, $t_{on}=100$ μs and $t_{off}=4000$ μs. The plasma power and pulse duty cycles employed in this study were chosen on the basis of *n*-factorial experimental design and then simplex optimisation. For comparative purposes, continuous wave plasma polymer films were deposited at 10 W. The notation used in this article for describing plasma co-polymerization follows the sequence in which the two monomers were introduced into the plasma chamber and their respective pressure settings. For example, $AA_{0.2}AL_{0.1}$ corresponds to the introduction of 0.2 mbar acrylic acid vapour into the chamber, and then the opening up of allylamine to give a total pressure of 0.3 mbar (0.2 + 0.1 mbar). The plasma polymer films were deposited onto glass slides (ultrasonically cleaned in a 1:1 solvent mixture of cyclohexane/propan-2-ol) for XPS analysis, potassium bromide powder for infrared analysis, and biaxial oriented polypropylene films (UCB) for gas permeation measurements.

A Kratos ES300 electron spectrometer equipped with a Mg K_α X-ray source (1253.6 eV), and a concentric hemispherical analyser was used for XPS analysis. Photoemitted electrons were collected at a take-off angle of 30° from the substrate normal, with electron detection in the fixed retarding ratio (FRR, 22:1) mode. XPS spectra were accumulated on an interfaced PC computer and fitted using a Marquardt minimisation algorithm with Gaussian peaks all having the same full-width-at-half-maximum (FWHM) [19]. Instrument sensitivity factors using reference chemical standards were taken as C (1s):O (1s):Si (2p):N (1s) equals 1.00:0.57:0.72:0.74.

Transmission infrared spectra were acquired over the 600–4000 cm^{-1} wavenumber range at a resolution of 4 cm^{-1} using a Mattson Polaris spectrometer. Hundred scans were averaged in conjunction with background subtraction.

The polymer film growth rate was measured with a quartz crystal thickness monitor (Kronos, Inc. Model QM-331) located in the centre of the plasma reactor.

Gas permeation measurements were acquired using a mass spectrometry apparatus [20]. This comprised placing a piece of coated polypropylene substrate between two drilled-out stainless steel flanges and a viton gasket. This assembly was attached to a UHV chamber via a gate valve (base pressure of 7×10^{-10} mbar) with the coated side of the polymer film exposed to an oxygen (BOC, 99.998%) pressure of 1316 mbar. A UHV ion gauge (Vacuum Generators, VIG 24) and a quadrupole mass spectrometer (Vacuum Generators SX200) interfaced to a PC computer were used to monitor the permeant pressure drop across the substrate. The quadrupole mass spectrometer's response per unit pressure was independently calculated by introducing oxygen directly into the chamber via a leak valve and recording the mass spectrum at a predetermined pressure of 5×10^{-7} mbar (taking into account ion-gauge sensitivity factors [21]). This was then used to calculate the mean equilibrium permeant partial pressure (MEPPP) of oxygen [22]. Finally, the barrier improvement factor (BIF) for each

Table 1
XPS elemental composition of pulsed plasma deposited polymer films (unless otherwise indicated)

Precursor(s)	%C (±3.0)	%Si (±0.1)	%O (±3.7)	%N		
				Total (±0.6)	Amine/amide (±0.4)	Ammonium salt (±0.6)
Acrylic acid (AA)	63.2	0.0	36.8	0.0	0.0	0.0
Allylamine (AL)	71.4	2.4	6.0	20.1	18.5	1.6
$AA_{0.15}AL_{0.15}$	68.1	0.0	16.9	15.0	8.0	7.0
$AA_{0.2}AL_{0.1}$	66.9	0.0	23.3	9.8	2.5	7.3
$AA_{0.2}AL_{0.1}$ (CW)	73.2	0.0	14.8	12.0	8.7	3.3

sample was determined by referencing with respect to the MEPPP value measured for uncoated polypropylene film.

3. Results and discussion

Continuous and pulsed plasma polymerization of the individual and mixtures of acrylic acid and allylamine monomers were compared, Fig. 1 and Table 1. The C (1s) XPS envelopes of acrylic acid and allylamine pulsed plasma polymers are similar in appearance to those reported previously [23–25]. In the case of salt formation, the different types of nitrogen environments can be estimated by fitting the N (1s) XPS envelope: [26–28] N–C (amine)/N–C=O (amide) at 399.4–400.3 eV, and N (ammonium salt) at 401.4–401.7 eV, Fig. 1. The small amount of ammonium salt detected in the case of the pure allylamine pulsed plasma deposited films is attributed to post-treatment adsorption of atmospheric CO_2 [29,30]. It is of interest to note that pulsed plasma deposition of poly(allylamine) gives rise to a high level of structural retention in contrast to continuous wave conditions [31] (over 100% enhancement in N/C XPS ratio). Pulsed plasma polymerization of $AA_{0.2}AL_{0.1}$ monomer mixtures gives rise to the largest amount of ammonium salt formation, Table 1. The corresponding experiment using continuous wave plasma conditions produced films with markedly different chemical characteristics, Table 1. This is evident from the accompanying shift in N (1s) peak shape towards lower XPS binding energies attributable to the formation of less ammonium salt centres.

Table 2
Assignment of infrared spectra [33–35]

Wavenumber/cm^{-1}	Assignment	Symbol
1705–1720	C=O stretching vibrations	■
1599–1638	N–H bending vibrations	
1636–1638	Amide I band	
1636–1642	C=C stretching vibrations	●
1638–1674	C=N stretching vibrations	
1562–1576	Asymmetrical CO_2^- stretching vibrations	♦
1454–1456	CH_2 bending vibrations	
1435	C–O–H bending vibrations	
1391–1406	Symmetrical CO_2^- stretching vibrations	♦
1244–1300	C–O stretching vibrations	
986–995	*trans*-CH= wagging	●
912	CH_2= wagging	
831	NH_2 wagging	

Infrared spectra obtained for the pulsed plasma polymer films deposited from the individual precursors displayed strong similarities with those reported for the monomers, Table 2 and Fig. 2. For instance, in the case of pulsed plasma polymerized acrylic acid, the presence of a narrow absorption band at 1720 cm^{-1} (C=O stretch) is indicative of high levels of carboxylic acid group retention. Whilst a broad peak at 1638 cm^{-1} (N–H bend) is observed for pulsed plasma deposited allylamine films. For both precursors, the disappearance of alkene absorption bands at 1636–1642 cm^{-1} (C=C stretch), 986–995 cm^{-1} (*trans*-CH= wag), and 912 cm^{-1} (CH_2= wag) correlates to the opening of the carbon–carbon double bonds during plasma polymerisation.

Continuous wave and pulsed plasma deposition of $AA_{0.2}AL_{0.1}$ mixtures gives rise to a number of similar infrared features, Fig. 2. The carbon–carbon double bonds has

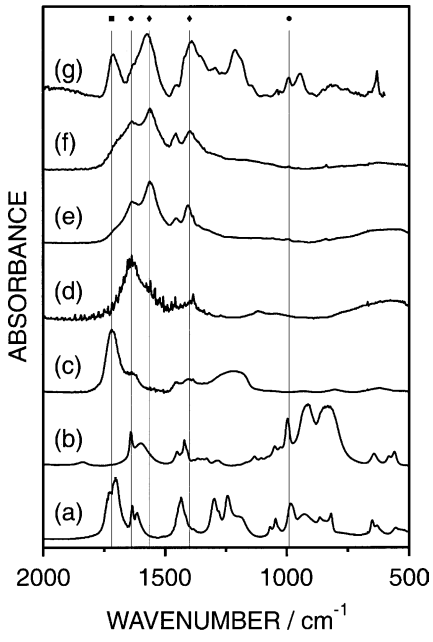

Fig. 2. Infrared spectra: (a) Acrylic acid, (b) allylamine, (c) acrylic acid pulsed plasma polymer, (d) allylamine pulsed plasma polymer, (e) acrylic acid (0.2 mbar)+allylamine (0.1 mbar) pulsed plasma polymer, (f) acrylic acid (0.2 mbar)+allylamine (0.1 mbar) continuous wave plasma polymer, and (g) pure acrylic acid+allylamine liquid mixture (1:1 molar ratio).

Table 3
Oxygen permeation measurements

Sample	MEPPP (10^{-8})	BIF[a]	Thickness/nm	Deposition rate/1×10^{-8} g s^{-1}
o-PP (reference sample)	29.1±1.3	1.0	–	–
Pulsed deposited allylamine	18.6±5.4	1.6	101.9±2.5	0.39
Pulsed deposited acrylic acid	4.3±2.7	6.8	253.4±86.8[b]	2.53
Pulsed deposited $AA_{0.2}AL_{0.1}$	2.9±1.8	10.0	52.1±1.1	2.91
CW deposited $AA_{0.2}AL_{0.1}$	21.4±3.3	1.4	102.6±4.0	4.34

[a] Barrier improvement factor.
[b] The large variation can be attributed to water absorption from the laboratory atmosphere as seen by the quartz crystal thickness monitor [36].

disappeared, and the absorption band at 1705–1720 cm^{-1} (C=O stretch) characteristic of carboxylic acid groups (associated with acrylic acid) is absent. Instead two new carboxylate group (salt) peaks at 1562–1576 cm^{-1} (asymmetrical CO_2^-) and 1391–1406 cm^{-1} (symmetrical CO_2^-) can be identified. In the case of the pulsed plasma polymer films, these infrared absorption features are found to be more intense relative to the methylene band at 1454–1456 cm^{-1} as compared to continuous wave conditions (thereby confirming the findings provided by XPS analysis). The assignment made for the carboxylate salt infrared absorption peak was confirmed by characterizing a 1:1 prepared liquid mixture of acrylic acid/allylamine.

These structural differences between continuous wave versus pulsed plasma deposited films was exemplified by undertaking gas barrier measurements. Oxygen gas permeation for the latter displayed a 10-fold improvement in gas barrier for $AA_{0.2}AL_{0.1}$ precursor mixtures, Table 3, whereas the corresponding film prepared under continuous wave conditions gave rise to no such improvement. The low BIF for pulsed plasma deposited poly(allylamine) onto polypropylene film can be attributed to pinholes in the coating as indicated by the presence of a Si (2p) XPS signal in the case of a glass substrate, Table 1.

Good structural retention (i.e. pulsed plasmachemical deposition) appears to be the key factor for making polymeric ammonium salt films which exhibit high gas barrier. Two simultaneous film formation mechanisms are envisaged to be in operation during pulsed plasma deposition: Firstly there is carbon–carbon bond formation via chain growth polymerization of the alkene groups contained in the precursor molecules; also there is concomitant salt formation via acid–base interactions between the respective carboxylic acid and amine centres prior to, during, and following oligomerization. The reason for poor salt formation (and hence high gas permeability) during the more energetic continuous wave conditions is due to extensive fragmentation and rearrangement of the precursor molecules within the electrical discharge.

The prerequisite for ammonium salt formation needed to achieve good gas barrier properties is consistent with previous solution phase chemistries [32] where, for example, mixtures of polyethylenimine with unsaturated dicarboxylic acids (such as itaconic, fumaric etc.) have been reported. Such intermolecular ionic interactions between amine and carboxylic groups present in the deposited plasma polymer film promote the formation of a closely packed gas impermeable structure.

4. Conclusions

Pulsed plasma co-polymerisation of acrylic acid with allylamine leads to the deposition of polymeric ammonium carboxylate salt films. These structurally well-defined layers display a significant improvement in gas barrier properties.

Acknowledgements

C. G. Spanos would like to thank Dow Corning for financial support and J. P. S. Badyal is grateful to EPSRC for an advanced research fellowship.

References

[1] Choi JO, Tyrell J. Patent EP 547555; 1993.
[2] Yamaguchi S, Yokoi T, Shioji S, Irie Y, Fujiwara T. Patent EP 396303; 1990.
[3] Nigam A. Patent WO 9954143; 1999.
[4] Dal'molin H, Maitre E, Vovelle L. Patent WO 9731782; 1997.
[5] Bader H, Keil KH, Rueppel D, Schlingmann M, Walch, A. Patent EP 280155; 1988.
[6] Iwane H, Okano K, Nakamura A. Patent JP 10175930; 1998.
[7] Yasuda H. Plasma polymerization. London: Academic Press; 1985.
[8] Garbassi F, Morra M, Occhiello E. Polymer surfaces—from physics to technology. Chichester, UK: Wiley; 1994.
[9] Hynes AM, Badyal JPS. Chem Mater 1998;10:2177.
[10] Panchalingam V, Chen X, Savage CR, Timmons RB, Eberhart C. J Appl Polym Sci: Appl Polym Symp 1994;54:123.
[11] Coulson SR, Woodward IS, Brewer SA, Willis C, Badyal JPS. Chem Mater 2000;12:2031.
[12] Tarducci C, Brewer SA, Willis C, Badyal JPS. Chem Mater 2000;12:1884.
[13] Ryan ME, Hynes AM, Badyal JPS. Chem Mater 1996;8:37.
[14] Hutton SJ, Crowther JM, Badyal JPS. Chem Mater 2000;12:2282.
[15] Tarducci C, Schofield WCE, Brewer S, Willis C, Badyal JPS. Chem Mater 2001;13:1800.
[16] Tarducci C, Schofield WCE, Brewer SA, Willis C, Badyal JPS. Chem Mater 2002;14:2541.
[17] Rimsch CL, Chem XL, Panchalingam V, Savage CR, Wang JH, Eberhart RC, et al. Abstr Pap Am Chem Soc Polym 1995;209:141.
[18] Savage CR, Timmons RB. Chem Mater 1991;3:575.

[19] Johanson G, Hedman J, Berndtsson A, Klasson M, Nilsson R. J Electron Spectrosc 1973;2:295.
[20] Barker CP, Kochem KH, Revell KM, Kelly RSA, Badyal JPS. Thin Solid Films 1995;259:46.
[21] Pressure measurement technical information, Vacuum Generators, Hastings, UK.
[22] Crank J, Park GS. In: Crank J, Park GS, editors. Diffusion in polymers. London: Academic Press; 1968 [chapter 1].
[23] Beamson G, Briggs D. High resolution XPS of organic polymers. The Scienta ESCA 300 database. Chichester, UK: Wiley; 1992, p. 53.
[24] Hutton SJ, Crowther JM, Badyal JPS. Chem Mater 2000;12:2282.
[25] Calderon JG, Harsch A, Gross GW, Timmons RB. J Biomed Mater Res 1998;42:597.
[26] Moulder JF, Stickle WF, Sobol PE, Bomben KD. In: Chastain J, editor. In handbook of X-ray photoelectron spectroscopy. Minnesota, MN: Perkin-Elmer Corporation; 1992.
[27] Beamson G, Briggs D. High resolution XPS of organic polymers: The Scienta ESCA300 database. New York: Wiley; 1992.
[28] Jousseaume V, Morsli M, Bonnet A, Lefrant S. J Appl Polym Sci 1998;67:1209.
[29] Williamson WH. Patent US 3961018; 1976.
[30] Chakraborty AK, Bischoff KB, Astarita G, Damewood Jr JR. J Am Chem Soc 1988;110:6947.
[31] Whittle JD, Barton D, Alexander MR, Short RD. Chem Commun 2003;1766.
[32] Wyman JE, Rangwalla I, Merlin PJ, Futter D, Power G, Branch K. Patent WO 9831719; 1998.
[33] Silverstein RM, Bassler GC, Morrill TC. Spectroscopic identification of organic compounds. Singapore: Wiley; 1991.
[34] Lin-Vien D, Colthup NB, Fateley WG, Grasselli JG. The handbook of infrared and characteristics of organic molecules. San Diego, CA: Academic Press; 1991.
[35] Bellamy LJ. The infrared spectra of complex molecules. London: Chapman and Hall; 1975.
[36] Alexander MR, Duc TM. Polymer 1999;40:5479.